PAPER Special Section on VLSI Design and CAD Algorithms

Second-Order Polynomial Expressions for On-Chip Interconnect Capacitance

Atsushi KUROKAWA[†a)], **Masanori HASHIMOTO**[††], ***Members***, **Akira KASEBE**[†††], ***Nonmember***, **Zhangcai HUANG**[††††], **Yun YANG**[††††], ***Student Members***, **Yasuaki INOUE**[††††], ***Member***, **Ryosuke INAGAKI**[†,††††], ***Student Member***, ***and*** **Hiroo MASUDA**[†], ***Member***

SUMMARY Simple closed-form expressions for efficiently calculating on-chip interconnect capacitances are presented. The formulas are expressed with second-order polynomial functions which do not include exponential functions. The runtime of the proposed formulas is about 2–10 times faster than those of existing formulas. The root mean square (RMS) errors of the proposed formulas are within 1.5%, 1.3%, 3.1%, and 4.6% of the results obtained by a field solver for structures with one line above a ground plane, one line between ground planes, three lines above a ground plane, and three lines between ground planes, respectively. The proposed formulas are also superior in accuracy to existing formulas.

key words: *capacitance formula, capacitance calculation, capacitance extraction, interconnect capacitance*

1. Introduction

In ASIC/SoC design, interconnects have taken a significant role in timing closure. Estimating parasitic interconnect capacitance easily and accurately is becoming more and more essential. Many closed-form expressions for calculating interconnect capacitances have been reported [1]–[7]. In our experience with real LSI designs, we have effectively utilized such capacitance formulas for a long time, especially Sakurai-Tamaru model [1]. Some of the existing formulas are limited to a structure with one line above a ground plane [5]–[7]. Comparisons of capacitances obtained by some formulas have been also reported [8], [9]. Crosstalk noise, which is the main issue for on-chip signal integrity, has become more and more significant. The models of Sakurai et al. [1], [2] are adjusted to account for structures with two and three parallel lines by considering the coupling capacitance. These models, however, apply only to a ground plane below parallel lines. Models for ground planes above and below three parallel lines have been developed by Chern et al. [3] and Wong et al. [4]. A technique for efficiently extracting interconnect capacitances of VLSI circuits in a design flow has also been reported [10]. Most of the formulas in the above papers are expressed as exponential functions or with complicated decimal orders. Moreover, the results calculated by using the existing formulas may include with more than 50% error. With the evolution of technology, the geometries of cross-sectional structures are changing. Existing formulas often cover the typical geometries when they were developed. Therefore, the coefficients in the formulas could be improved in accuracy by refitting according to recent wire structures.

In this paper, we present simple closed-form expressions for efficiently calculating on-chip interconnect capacitances. For the structures of one line above a ground plane, one line between ground planes, and three lines between ground planes, we create four formulas. These formulas are expressed as polynomial functions of second-order, without complicated exponential functions. The formulas were obtained by using the response surface methodology (RSM) [11]–[13]. In general, a low-order polynomial approximation function can achieve high accuracy when the range of each parameter is narrow. In the structures of three lines, the coupling capacitance becomes very small as the spacing becomes large. According to our experiences, a second-order polynomial function can not give reasonably accurate capacitance when the parameter range of interconnect structure is wide. We thus limited the applicable range of formulas to triple spacing (double pitch) from a viewpoint of practical use. The double pitch is generally used for crosstalk noise avoidance, and is included in the valid range of the proposed formulas. On the other hand, as the spacing becomes larger than triple spacing, the accuracy gets worse and unacceptable. However, when spacing between lines is very wide, the capacitance for three lines is close to that for one line. Though the valid range of structural parameters is limited, the formulas are useful for calculating interconnect capacitances for the most cases of crosstalk noise analysis, IR-drop analysis, interconnect design for high-speed signal propagation, and so on. The proposed formulas have the following advantages:

- Simple expressions with second-order polynomials, which yield shorter calculation time.
- Including a structure with one line between ground planes, which has not yet been reported.
- Compatibility with current and future technologies.
- Reasonable accuracy (higher than most existing formulas).
- Easy differentiation that is suitable for wire geometry

Manuscript received March 14, 2005.
Manuscript revised June 9, 2005.
Final manuscript received August 2, 2005.

[†]The authors are with STARC, Yokohama-shi, 222-0033 Japan.
[††]The author is with Osaka University, Suita-shi, 565-0871 Japan.
[†††]The author is with Meitec Corp., Tokyo, 104-0061 Japan.
[††††]The authors are with Waseda University, Kitakyushu-shi, 808-0135 Japan.
a) E-mail: kurokawa@starc.or.jp

DOI: 10.1093/ietfec/e88–a.12.3453

optimization and variational analysis for manufacturing fluctuation.

The remainder of the paper is organized as follows. Section 2 reviews interconnect capacitances and existing closed-form recessions. Section 3 presents a set of formulas for interconnect capacitance obtained by RSM. Section 4 shows experimental results demonstrating comparisons with the existing formulas, and we conclude the paper in Sect. 5.

2. Preliminaries

Before introducing the proposed formulas, we discuss existing formulas and interconnect structures. We also analyze the sensitivity of interconnect capacitance with respect to each geometric parameter.

2.1 Interconnect Structures

Figure 1 shows cross sections of typical interconnect structures, where w is the line width, t is the thickness, h is the height and s is the spacing. The formulas presented in this paper focus on the four structures shown in the figure. The structures, consisting of one line above a ground plane, one line between ground planes, three lines above a ground plane, and three lines between ground planes, are designated as 1L1G, 1L2G, 3L1G, and 3L2G, respectively. Table 1 lists the interconnect parameters of ITRS 90–22 nm technologies [14]. The aspect ratio is calculated assuming that the wire width is a minimum at each layer. This work aims to develop simple yet accurate closed-form expressions that can cover the interconnect geometries in Table 1.

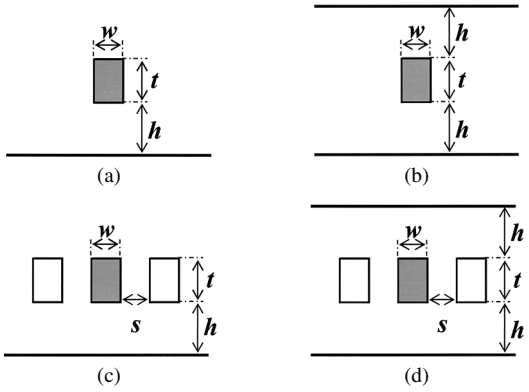

Fig. 1 Interconnect structures: (a) one line above a ground plane (1L1G), (b) one line between ground planes (1L2G), (c) three lines above a ground plane (3L1G), and (d) three lines between ground planes (3L2G).

Table 1 Aspect ratios of interconnect structures of ITRS 90–22 nm technologies.

Year	2004	2007	2010	2013	2016
Technology (nm)	90	65	45	35	22
Wire A/R	1.7–2.1	1.7–2.2	1.8–2.3	1.9–2.4	2.0–2.5
Via A/R	1.5–1.9	1.6–2.0	1.6–2.1	1.7–2.2	1.8–2.3

2.2 Existing Formulas

Many formulas for calculating interconnect capacitances have been reported [1]–[7]. The accuracy of capacitance formulas for one line above a ground plane in Fig. 1(a) was compared in [8]. However, the accuracy of capacitance formulas for three lines was not compared yet. For example, formulas for three lines above a ground plane (3L1G) in Fig. 1(c) are as follows.

Sakurai et al. models [1], [2] for 3L1G are

$$C_t=\varepsilon\cdot l\cdot\left[2.80\left(\frac{t}{h}\right)^{0.222}+1.15\left(\frac{w}{h}\right)+2\left(0.83\left(\frac{t}{h}\right)-0.07\left(\frac{t}{h}\right)^{0.222}+0.03\left(\frac{w}{h}\right)\right)\left(\frac{s}{h}\right)^{-1.34}\right], \tag{1}$$

$$C_c=\varepsilon\cdot l\cdot\left[\left(1.93\left(\frac{t}{h}\right)^{1.1}+1.14\left(\frac{w}{h}\right)^{0.31}\right)\cdot\left(\frac{s}{h}+0.51\right)^{-1.45}\right], \tag{2}$$

$$C_g=C_t-2C_c, \tag{3}$$

where the relative error for C_t is less than 10% for $0.3 < t/h < 10$, $0.3 < w/h < 10$, and $0.5 < s/h < 10$, and the relative error for C_c is less than 15% for $0.3 < t/h < 3$, $0.3 < w/h < 3$, and $0.3 < s/h < 3$.

Chern et al. models [3] are

$$C_g=\varepsilon\cdot l\cdot\left[\frac{w}{h}+3.28\left(\frac{t}{t+2h}\right)^{0.023}\left(\frac{s}{s+2h}\right)^{1.16}\right], \tag{4}$$

$$C_c=\varepsilon\cdot l\cdot\left[1.064\left(\frac{t}{s}\right)\left(\frac{t+2h}{t+2h+0.5s}\right)^{0.695}+\left(\frac{w}{w+0.8s}\right)^{1.4148}\left(\frac{t+2h}{t+2h+0.5s}\right)^{0.804}+0.831\left(\frac{w}{w+0.8s}\right)^{0.055}\left(\frac{2h}{2h+0.5s}\right)^{3.542}\right], \tag{5}$$

$$C_t=C_g+2C_c, \tag{6}$$

where the valid ranges are $0.3 \le t/h \le 10$, $0.3 \le w/h \le 10$, and $0.3 \le s/h \le 10$.

Wong et al. models [4] are

$$C_g=\varepsilon\cdot l\cdot\left[\frac{w}{h}+2.217\left(\frac{s}{s+0.702h}\right)^{3.193}+1.171\left(\frac{s}{s+1.510h}\right)^{0.7642}\left(\frac{t}{t+4.532h}\right)^{0.1204}\right], \tag{7}$$

$$C_c=\varepsilon\cdot l\cdot\left[1.144\left(\frac{t}{s}\right)\left(\frac{h}{h+2.059s}\right)^{0.0944}+0.7428\left(\frac{w}{w+1.592s}\right)^{1.144}+1.158\left(\frac{w}{w+1.874s}\right)^{0.1612}\left(\frac{h}{h+0.9801s}\right)^{1.179}\right], \tag{8}$$

Table 2 Efficient ranges of the existing formulas described in each paper.

Structure	Formula	Capacitance	Range
1L1G	Sakurai et al. [1]	C_t	$0.3 < \frac{t}{h} < 30,\ \ 0.3 < \frac{w}{h} < 30$
	Elmasry [5]	C_t	—
	Yuan et al. [6]	C_t	—
	Meijs et al. [7]	C_t	$\frac{t}{h} \le 10,\ \ 0.3 \le \frac{w}{h}$
3L1G	Sakurai [2]	C_t	$0.3 < \frac{t}{h} < 10,\ \ 0.3 < \frac{w}{h} < 10,\ \ 0.5 < \frac{s}{h} < 10$
		C_c	$0.3 < \frac{t}{h} < 3,\ \ 0.3 < \frac{w}{h} < 3,\ \ 0.3 < \frac{s}{h} < 3$
	Chern et al. [3]	C_g, C_c	$0.3 \le \frac{t}{h} \le 10,\ \ 0.3 \le \frac{w}{h} \le 10,\ \ 0.3 \le \frac{s}{h} \le 10$
	Wong et al. [4]	C_g, C_c	$0.15 < t < 1.2,\ \ 0.16 < h < 2.71,\ \ 0.16 < s < 10,\ \ 0.16 < w < 2$
3L2G	Chern et al. [3]	C_g, C_c	$0.3 \le \frac{t}{h} \le 10,\ \ 0.3 \le \frac{w}{h} \le 10,\ \ 0.3 \le \frac{s}{h} \le 10$
	Wong et al. [4]	C_g, C_c	$0.15 < t < 1.2,\ \ 0.16 < h < 2.71,\ \ 0.16 < s < 10,\ \ 0.16 < w < 2$

$$C_t = C_g + 2C_c, \tag{9}$$

where the ranges are $0.15 < t < 1.2$, $0.16 < h < 2.71$, $0.16 < s < 10$, and $0.16 < w < 2$ with units of micrometers.

Here, C_g is the ground capacitance, C_c is the coupling capacitance, ε is the permittivity, l is the line length, and the unit of C_g and C_c is Farad. Table 2 lists the effective ranges of existing formulas described in each paper. The applicable interconnect structures of these formulas seem to include a large variety at a glance, however, some basic interconnect structures in recent advanced technologies are not covered. For example, in Sakurai and Chern models, due to high aspect ratio as shown in Table 1, the structure with minimum spacing in the second metal layer above a ground plane is out of effective range. On the other hand, the proposed formulas are derived based on the prediction in ITRS roadmap, and hence the compatibility of the proposed formulas with advanced technologies is advantaged.

Another advantage of the proposed formulas is less computational cost, which comes from expressions composed of second-order polynomials, whereas existing formulas include complicated exponential functions. The runtime and accuracy of existing formulas are compared with those of the proposed formulas in Sect. 4.

3. Proposed Formulas

In this section, we present the new formulas for calculating interconnect capacitance.

3.1 Sensitivity Analysis for Predictor Variable Selection

To create capacitance formulas with higher accuracy, it is important to understand the sensitivity of the interconnect capacitance with respect to parameter variations in each structure. In this subsection, by using the intermediate interconnect parameters of ITRS 90-nm technology, we clarify the sensitivity characteristics of the interconnect capacitance. Figure 2 shows the results of sensitivity analysis for various parameters obtained by a field solver [15] for the 3L2G structure shown in Fig. 1(d). C_g is the ground capacitance between the objective line and the ground plane. C_c is the coupling capacitance between the objective line and the neighboring line. We can observe the following relationships for each parameter:

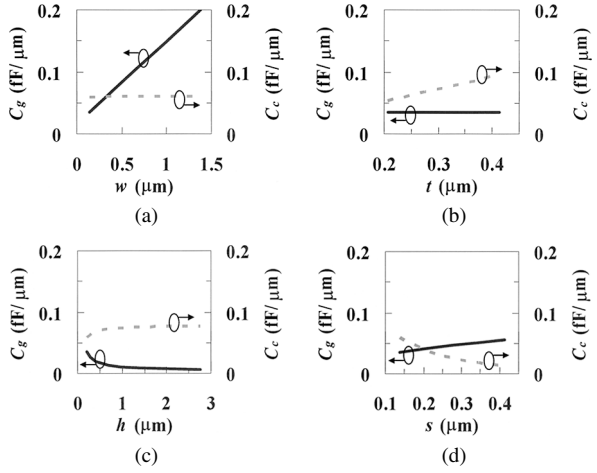

Fig. 2 Results of sensitivity analysis for each type of interconnect parameter variation: (a) dependence on w, (b) dependence on t, (c) dependence on h, and (d) dependence on s.

- The ground capacitance, C_g, increased almost linearly with w, did not vary with t, decreased in inverse proportion to h, and increased slightly with s.
- The coupling capacitance, C_c, did not vary with w, increased almost linearly with t, increased slightly with h, and decreased in inverse proportion to s.

The results of the sensitivity analysis were utilized in determining the predictor variables required for developing the new formulas for interconnect capacitance.

3.2 Applicable Structures

If the geometric parameters of the cross sections in two interconnect structures have a similarity relationship, the capacitances are the same. Figure 3 shows illustrations of an

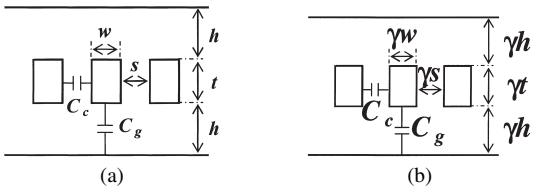

Fig. 3 Capacitances of similar cross sections: (a) an original structure, and (b) the same structure shrunk by a factor of γ.

Table 3 Applicable ranges of the proposed formulas.

Parameter	Applicable range	Values used for analysis
Width, w	1–10	1 steps
Thickness, t	1.5–3	0.5 steps
Height, h	1.5–20	0.5 steps
Spacing, s	1–3	0.5 steps

original cross section and the same cross section shrunk by a factor of γ. The respective values of C_g and C_c in Fig. 3(a) are the same as those in Fig. 3(b). Based on such relationships, we can create dimensionless capacitance formulas that are independent of the physical values of the interconnect parameters. Table 3 lists the values of the geometric parameters used in our analysis and the applicable ranges of the developed formulas. The values are relative ratios (dimensionless). The applicable structures in Table 3 correspond to the current and future technologies listed in Table 1.

3.3 Creation of New Formulas

The proposed formulas are expressed as polynomial functions obtained by the response surface methodology. The response surface function (RSF) essentially corresponds to Taylor expansion of an exact function. The general form of the RSF is

$$y = \beta_0 + \sum_{i=1}^{k} \beta_i x_i + \sum_{i=1}^{k} \sum_{j \geq i}^{k} \beta_{ij} x_i x_j + \cdots, \tag{10}$$

where β is the coefficient, x is the predictor variable, and k is the number of variables. We develop the capacitance formulas by using the terms up to the second order. The capacitance formulas are created by the following procedure:

1. Determine the cross-sectional structures and parameter ranges.
2. Extract the capacitances of each structure by using a field solver.
3. Fit the coefficients of each second-order polynomial by using the RSM.
4. Eliminate the variables that hardly influence the capacitance value according to the results of regression analysis.
5. Determine the formulas for each structure.

The forms of the predictor variables are determined based on the physics and the results of the sensitivity analysis shown in Fig. 2. For example, we determined that the set of predictor variables for the structure shown in Fig. 1(d) is $(w, t, 1/h, s)$ for C_g and $(w, t, h, 1/s)$ for C_c. The basic forms for the capacitances are

$$C_g = \varepsilon \cdot l \cdot f(w, t, 1/h, s), \tag{11}$$

$$C_c = \varepsilon \cdot l \cdot g(w, t, h, 1/s), \tag{12}$$

$$C_t = 2(C_g + C_c), \tag{13}$$

where ϵ is the dielectric permittivity, l is the line length, and C_t is the total capacitance. The full quadratic polynomial function, $g_0(w, t, h, 1/s)$ for C_c is

$$\begin{aligned} g_0(w, t, h, 1/s) = {} & \beta_0 + \beta_1 \frac{w}{\alpha} + \beta_2 \frac{t}{\alpha} + \beta_3 \frac{h}{\alpha} \\ & + \beta_4 \frac{\alpha}{s} + \beta_{11} \left(\frac{w}{\alpha}\right)^2 + \beta_{12} \frac{wt}{\alpha^2} + \beta_{13} \frac{wh}{\alpha^2} \\ & + \beta_{14} \frac{w}{s} + \beta_{22} \left(\frac{t}{\alpha}\right)^2 + \beta_{23} \frac{th}{\alpha^2} + \beta_{24} \frac{t}{s} \\ & + \beta_{33} \left(\frac{h}{\alpha}\right)^2 + \beta_{34} \frac{h}{s} + \beta_{44} \left(\frac{\alpha}{s}\right)^2, \end{aligned} \tag{14}$$

where α is the factor for converting the dimensions. It is important that the values converted by α are within the ratios shown in Table 3. In general, α should be the minimum line width in the objective metal layer. As the expression of (14) is redundant, we eliminate the terms that have small sensitivity. As a result, the terms of β_2, β_{11}, β_{12}, β_{14}, β_{22}, β_{23}, and β_{34} are eliminated. Figure 4 plots the results of regression analysis for the improved $g(w, t, h, 1/s)$ formula. The adjusted R (multiple correlation coefficient) square was 0.99, indicating a very high degree of parameter fitting.

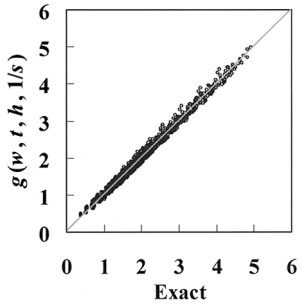

Fig. 4 Results of regression analysis for a coupling capacitance formula.

3.4 Set of Proposed Formulas

We now present the developed set of formulas for interconnect capacitance. Tables 4 and 5 list the coefficients of each formula.

Capacitance for one line (1L1G, 1L2G):

$$\begin{aligned} C_g = {} & \varepsilon \cdot l \cdot \left(\beta_0 + \beta_1 \frac{w}{\alpha} + \beta_2 \frac{t}{\alpha} + \beta_3 \frac{\alpha}{h} + \beta_{11} \left(\frac{w}{\alpha}\right)^2 \right. \\ & \left. + \beta_{13} \frac{w}{h} + \beta_{23} \frac{t}{h} + \beta_{33} \left(\frac{\alpha}{h}\right)^2 \right). \end{aligned} \tag{15}$$

Capacitances for three lines (3L1G, 3L2G):

$$C_g = \varepsilon \cdot l \cdot \left(\beta_0 + \beta_1 \frac{w}{\alpha} + \beta_3 \frac{\alpha}{h} + \beta_4 \frac{s}{\alpha} + \beta_{11}\left(\frac{w}{\alpha}\right)^2 + \beta_{13}\frac{w}{h} + \beta_{14}\frac{ws}{\alpha^2} + \beta_{34}\frac{s}{h}\right), \quad (16)$$

$$C_c = \varepsilon \cdot l \cdot \left(\beta_0 + \beta_1 \frac{w}{\alpha} + \beta_3 \frac{h}{\alpha} + \beta_4 \frac{\alpha}{s} + \beta_{13}\frac{wh}{\alpha^2} + \beta_{24}\frac{t}{s} + \beta_{33}\left(\frac{h}{\alpha}\right)^2 + \beta_{44}\left(\frac{\alpha}{s}\right)^2\right). \quad (17)$$

If the heights of top ground layer and bottom ground layer are divided by h_t and h_b, respectively, Eq. (15) for 1L2G structure is reused as follows:

$$C_g = \varepsilon \cdot l \cdot \left(\beta_0 + \beta_1 \frac{w}{\alpha} + \beta_2 \frac{t}{\alpha} + \frac{\beta_3}{2}\frac{\alpha}{h_b} + \frac{\beta_3}{2}\frac{\alpha}{h_t} + \beta_{11}\left(\frac{w}{\alpha}\right)^2 + \frac{\beta_{13}}{2}\frac{w}{h_b} + \frac{\beta_{13}}{2}\frac{w}{h_t} + \frac{\beta_{23}}{2}\frac{t}{h_b} + \frac{\beta_{23}}{2}\frac{t}{h_t} + \frac{\beta_{33}}{2}\left(\frac{\alpha}{h_b}\right)^2 + \frac{\beta_{33}}{2}\left(\frac{\alpha}{h_t}\right)^2\right). \quad (18)$$

Similarly, Eqs. (16) and (17) for 3L2G become as follows:

$$C_g = \varepsilon \cdot l \cdot \left(\beta_0 + \beta_1 \frac{w}{\alpha} + \frac{\beta_3}{2}\frac{\alpha}{h_b} + \frac{\beta_3}{2}\frac{\alpha}{h_t} + \beta_4 \frac{s}{\alpha} + \beta_{11}\left(\frac{w}{\alpha}\right)^2 + \frac{\beta_{13}}{2}\frac{w}{h_b} + \frac{\beta_{13}}{2}\frac{w}{h_t} + \beta_{14}\frac{ws}{\alpha^2} + \frac{\beta_{34}}{2}\frac{s}{h_b} + \frac{\beta_{34}}{2}\frac{s}{h_t}\right), \quad (19)$$

$$C_c = \varepsilon \cdot l \cdot \left(\beta_0 + \beta_1 \frac{w}{\alpha} + \frac{\beta_3}{2}\frac{h_b}{\alpha} + \frac{\beta_3}{2}\frac{h_t}{\alpha} + \beta_4 \frac{\alpha}{s} + \frac{\beta_{13}}{2}\frac{wh_b}{\alpha^2} + \frac{\beta_{13}}{2}\frac{wh_t}{\alpha^2} + \beta_{24}\frac{t}{s} + \frac{\beta_{33}}{2}\left(\frac{h_b}{\alpha}\right)^2 + \frac{\beta_{33}}{2}\left(\frac{h_t}{\alpha}\right)^2 + \beta_{44}\left(\frac{\alpha}{s}\right)^2\right). \quad (20)$$

The capacitances of these formulas have a unit of Farad. The valid ranges with relative ratios of each parameter as shown in Table 3 are $1 \le w \le 10$, $1.5 \le t \le 3$, $1.5 \le h \le 20$, and $1 \le s \le 3$.

Table 4 Coefficients of the formulas for one line.

Coefficients for C_g		
Name	Value	
	1L1G	1L2G
β_0	1.1	0.639
β_1	0.0867	0.0248
β_2	0.106	0.066
β_3	4.03	1.83
β_{11}	−0.00381	−0.00116
β_{13}	1.03	0.98
β_{23}	0.305	0.345
β_{33}	−3.29	−1.48

Table 5 Coefficients of the formulas for three lines.

Coefficients for C_g			Coefficients for C_c		
Name	Value		Name	Value	
	3L1G	3L2G		3L1G	3L2G
β_0	0.251	0.119	β_0	−0.318	−0.779
β_1	0.00113	−0.02025	β_1	0.0469	−0.00206
β_3	0.294	0.143	β_3	0.0781	0.143
β_4	0.0574	0.0297	β_4	1.63	1.77
β_{11}	0.0000426	0.000696	β_{13}	0.00206	0.0042
β_{13}	1.01	1.02	β_{24}	1.01	1
β_{14}	−0.00136	0.000885	β_{33}	−0.00273	−0.00512
β_{34}	0.615	0.575	β_{44}	−0.608	−0.66

4. Evaluation of Runtime and Accuracy

We now demonstrate the validity of the proposed formulas. First, we compare the runtime required to calculate capacitances by using each formula. The evaluation has been executed on SunOS 5.6 (Ultra-80) with C language. The relative runtime values are computed assuming that the cputime by the proposed formula for 1L1G is one. For 3L1G and 3L2G, the total time of C_t, C_g, and C_c by each formula is evaluated. Table 6 shows the results of the relative runtime. We can see that the runtime of the proposed formulas is about 2–10 times shorter than those of existing formulas.

Next, we compare the accuracies of the proposed formulas and existing formulas. We evaluate the estimation error from the field solver results. Figure 5 plots the estimation error of ground capacitance C_g in 3L1G structure in Fig. 1(c). Similarly, Fig. 6 shows the results for coupling capacitance C_c in 3L1G structure. Figures 5(a)–(c) and 6(a)–(c) represent the estimation errors by Sakurai, Chern and Wong formulas, respectively. The geometric parameter range of interconnect structure for experiments is determined formula by formula such that both the proposed formula and the target formula are valid. Figures 5(d)–(f) and 6(d)–(f) show the estimation errors of the proposed formu-

Table 6 Relative runtime of each formula.

Structure	Formula	Relative runtime
1L1G	Sakurai et al. [1]	2.5
	Elmasry [5]	2.4
	Yuan et al. [6]	2.4
	Meijs et al. [7]	3.4
	Proposed	1.0
1L2G	Proposed	1.1
3L1G	Sakurai [2]	14.3
	Chern et al. [3]	17.1
	Wong et al. [4]	16.2
	Proposed	1.7
3L2G	Chern et al. [3]	13.1
	Wong et al. [4]	11.6
	Proposed	1.7

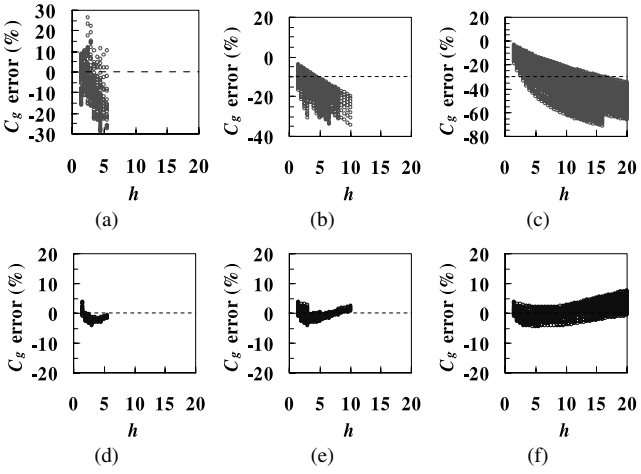

Fig. 5 Comparison of the C_g errors obtained by each formula for the 3L1G structure shown in Fig. 1(c): (a) Sakurai [2] in the range of No.4 in Table 7, (b) Chern et al. [3] in the range of No.5 in Table 7, (c) Wong et al. [4] in the range of No.6 in Table 7, (d) proposed formula in the range of No.4 in Table 7, (e) proposed formula in the range of No.5 in Table 7, and (f) proposed formula in the range of No.6 in Table 7.

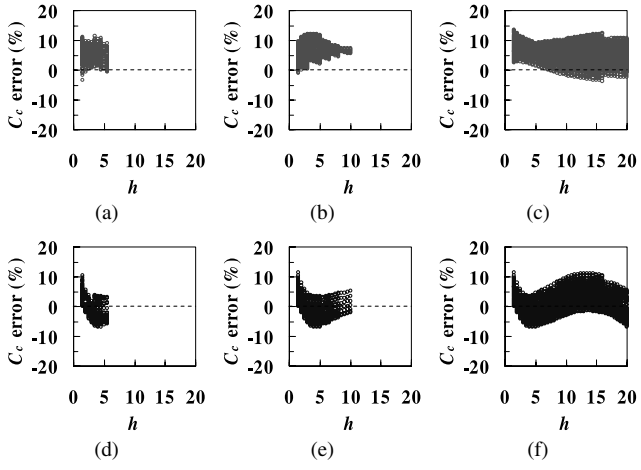

Fig. 6 Comparison of the C_c errors obtained by each formula for the 3L1G structure shown in Fig. 1(c): (a) Sakurai [2] in the range of No.4 in Table 7, (b) Chern et al. [3] in the range of No.5 in Table 7, (c) Wong et al. [4] in the range of No.6 in Table 7, (d) proposed formula in the range of No.4 in Table 7, (e) proposed formula in the range of No.5 in Table 7, and (f) proposed formula in the range of No.6 in Table 7.

las in the same parameter sets with (a-c) respectively, i.e. (a) and (d), (b) and (e), and (c) and (f) are evaluated in the same parameter range. The parameter ranges used for the experiments are summarized in Table 7.

We can see that the accuracy of the proposed formulas are superior to those of Sakurai, Chern and Wong formulas. Even for the structures in which existing formulas are valid, the estimation error can be above 30%, and it is unacceptably large.

Figure 7 plots the results of the total capacitance errors for the 3L2G structure in Fig. 1(d). The errors of the proposed formulas are smaller than those of Chern and Wong formulas. Tables 8–10 list the maximum errors and RMS errors of each formula in each common range. In most cases, the proposed formulas are superior to existing formulas in accuracy.

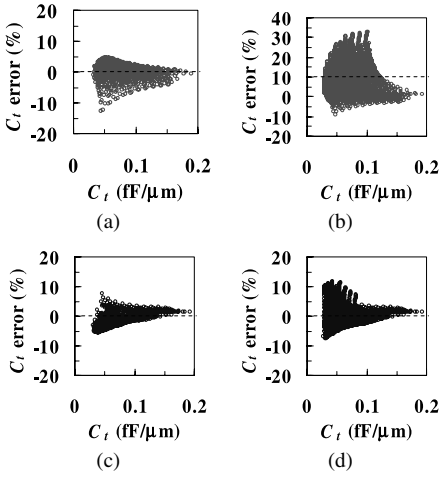

Fig. 7 Error distribution of the C_t obtained by each formula for the 3L2G structure shown in Fig. 1(d): (a) Chern et al. [3] in the range of No.5 in Table 7, (b) Wong et al. [4] in the range of No.6 in Table 7, (c) proposed formula in the range of No.5 in Table 7, and (d) proposed formula in the range of No.6 in Table 7.

Figure 8 shows the error distributions of the proposed formulas in the range of Table 3. Table 11 summarizes the accuracy of the proposed formulas. The maximum error of the formula for 1L1G is 4.6% and smaller than the other formulas. The maximum error of our formula for 1L2G is 5.9% and the accuracy is reasonable. The RMS errors of the proposed formulas for C_g and C_c are 2.0% and 3.1% for 3L1G, and 2.1% and 4.6% for 3L2G, respectively. The proposed formulas are simpler expressions, yet attain higher accuracy in the ranges shown in Table 3.

Here, we summarize features of the proposed formulas. First, we describe the valid ranges again. The valid ranges are $1 \leq w \leq 10$, $1.5 \leq t \leq 3$, $1.5 \leq h \leq 20$, and $1 \leq s \leq 3$. The accuracies within the ranges are, in each maximum error, about 4.6%, 5.9%, 11.3%, and 23.6% for 1L1G, 1L2G, 3L1G, and 3L2G as shown in Table 11. The accuracy is not guaranteed when structural parameters are out of range, and especially the accuracy is sensitive to spacing parameter. That is, the disadvantage is that applicable spacing range for three lines is narrow and is limited up to double pitch. The advantages are that 1) calculation time is 2.4 times faster than existing formulas as shown in Table 6, 2) formulas for a structure with one line between ground planes, which has not yet been reported, were also presented, 3) formulas correspond to interconnect structures for current and future technologies, 4) accuracy are reasonable and higher than most existing formulas in our range, and 5) formulas can be easily differentiated, which is suitable for wire geometry optimization and variational analysis for manufacturing fluctuation, because of second-order functions.

Table 7 Parameter ranges used for accuracy comparison. For each parameter value, h, t, and s are 0.5 steps and w is 1 steps.

Structure	Formula	Range	# of structures	Range No.
1L1G	Sakurai et al. [1]	$1.5 \le h \le 3$ & $1.5 \le t \le 3$ & $1 \le w \le 10$ $3.5 \le h \le 4.5$ & $1.5 \le t \le 3$ & $2 \le w \le 10$ $5 \le h \le 6.5$ & $2 \le t \le 3$ & $2 \le w \le 10$ $7 \le h \le 8$ & $2.5 \le t \le 3$ & $3 \le w \le 10$ $8.5 \le h \le 9.5$ & $t = 3$ & $3 \le w \le 10$	448	1
	Elmasry [5] Yuan et al. [6]	$1.5 \le h \le 20$ & $1.5 \le t \le 3$ & $1 \le w \le 10$	1520	2
	Meijs et al. [7]	$1.5 \le h \le 3$ & $1.5 \le t \le 3$ & $1 \le w \le 10$ $3.5 \le h \le 6.5$ & $1.5 \le t \le 3$ & $2 \le w \le 10$ $7 \le h \le 10$ & $1.5 \le t \le 3$ & $3 \le w \le 10$ $10.5 \le h \le 13$ & $1.5 \le t \le 3$ & $4 \le w \le 10$ $13.5 \le h \le 16.5$ & $1.5 \le t \le 3$ & $5 \le w \le 10$ $17 \le h \le 20$ & $1.5 \le t \le 3$ & $6 \le w \le 10$	1112	3
3L1G	Sakurai [2]	$h = 1.5$ & $1.5 \le t \le 3$ & $1 \le w \le 4$ & $1 \le s \le 3$ $h = 2$ & $1.5 \le t \le 3$ & $1 \le w \le 5$ & $1.5 \le s \le 3$ $h = 2.5$ & $1.5 \le t \le 3$ & $1 \le w \le 7$ & $1.5 \le s \le 3$ $h = 3$ & $1.5 \le t \le 3$ & $1 \le w \le 8$ & $2 \le s \le 3$ $h = 3.5$ & $1.5 \le t \le 3$ & $2 \le w \le 10$ & $2 \le s \le 3$ $4 \le h \le 4.5$ & $1.5 \le t \le 3$ & $2 \le w \le 10$ & $2.5 \le s \le 3$ $5 \le h \le 5.5$ & $2 \le t \le 3$ & $2 \le w \le 10$ & $s = 3$	674	4
3L1G 3L2G	Chern et al. [3]	$1.5 \le h \le 3$ & $1.5 \le t \le 3$ & $1 \le w \le 10$ & $1 \le s \le 3$ $3.5 \le h \le 5$ & $1.5 \le t \le 3$ & $2 \le w \le 10$ & $1.5 \le s \le 3$ $5.5 \le h \le 6.5$ & $2 \le t \le 3$ & $2 \le w \le 10$ & $2 \le s \le 3$ $7 \le h \le 8$ & $2.5 \le t \le 3$ & $3 \le w \le 10$ & $2.5 \le s \le 3$ $8.5 \le h \le 10$ & $t = 3$ & $3 \le w \le 10$ & $s = 3$	1747	5
	Wong et al. [4]	$1.5 \le h \le 16$ & $1.5 \le t \le 3$ & $1 \le w \le 10$ & $1 \le s \le 3$ $16.5 \le h \le 20$ & $1.5 \le t \le 3$ & $2 \le w \le 10$ & $1.5 \le s \le 3$	7152	6

Table 8 Accuracy comparison for the 1L1G.

Range No. in Table 7	Formula	C_t error (%)	
		Max	RMS
1	Sakurai et al. [1]	−4.1	1.8
	Proposed	3.9	1.2
2	Elmasry [5]	−87.3	61.2
	Yuan et al. [6]	−16.8	7.7
	Proposed	4.6	1.5
3	Meijs et al. [7]	−4.7	0.8
	Proposed	4.6	1.5

5. Conclusions

We have presented simple formulas for calculating interconnect capacitance. The formulas are expressed with second-order polynomial functions. The results obtained by the proposed formulas exhibit good accuracy.

The formulas for three lines presented in this paper are applicable for up to double spacing. To widen applicable parameter ranges using low-order polynomial function, for example, some formulas whose valid ranges are well separated are required. Our future work is to develop formulas of higher accuracy and more practical use.

Acknowledgments

We would like to thank Chang Wei Fong and Kazuya Sono of C-Tech Corp. for their helpful discussions.

References

[1] T. Sakurai and K. Tamaru, "Simple formulas for two- and three-dimensional capacitances," IEEE Trans. Electron Devices, vol.ED-30, no.2, pp.183–185, Feb. 1983.
[2] T. Sakurai, "Closed-form expressions for interconnection delay, coupling, and crosstalk in VLSI's," IEEE Trans. Electron Devices,

Table 9 Accuracy comparison for the 3L1G.

Range No. in Table 7	Formula	C_t error (%)		C_g error (%)		C_c error (%)	
		Max	RMS	Max	RMS	Max	RMS
4	Sakurai [2]	7.9	3.3	−29.0	11.5	11.4	5.9
	Proposed	6.2	2.7	−4.0	1.9	10.4	3.5
5	Chern et al. [3]	−7.8	1.4	−34.6	15.0	12.2	6.8
	Proposed	6.2	2.4	−4.0	1.5	11.3	3.3
6	Wong et al. [4]	7.0	2.4	−71.1	35.4	13.3	6.4
	Proposed	9.5	2.5	7.6	1.9	11.3	3.1

Table 10 Accuracy comparison for the 3L2G.

Range No. in Table 7	Formula	C_t error (%)		C_g error (%)		C_c error (%)	
		Max	RMS	Max	RMS	Max	RMS
5	Chern et al. [3]	−12.9	2.6	−10.1	1.7	−47.0	8.7
	Proposed	7.6	2.7	6.2	1.1	23.6	6.2
6	Wong et al. [4]	32.9	9.1	−64.8	18.0	40.5	14.0
	Proposed	11.8	3.0	−7.3	1.8	23.6	4.7

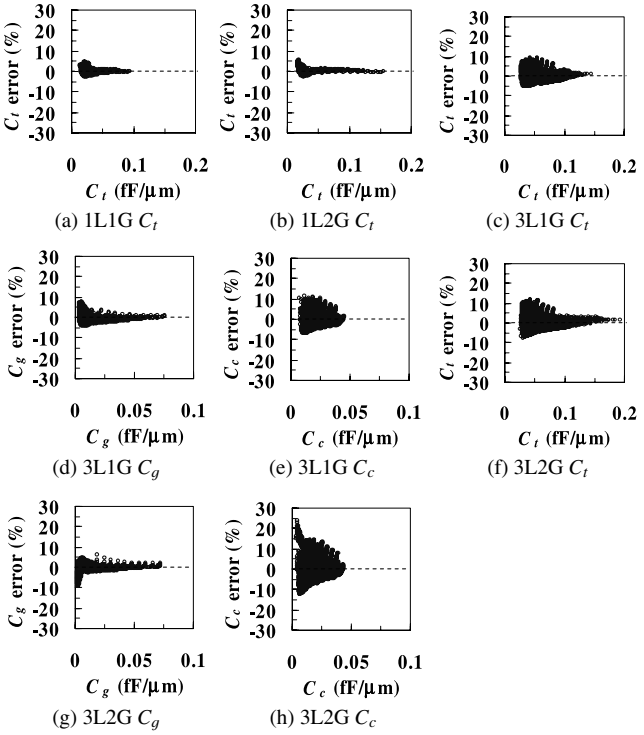

Fig. 8 Error distribution of the proposed formulas in the range of Table 3.

Table 11 Accuracy of the proposed formulas in the range of Table 3. The numbers of structures are 1520 for 1L1G and 1L2G, and 7600 for 3L1G and 3L2G.

Structure	C_t error (%)		C_g error (%)		C_c error (%)	
	Max	RMS	Max	RMS	Max	RMS
1L1G	4.6	1.5	—	—	—	—
1L2G	5.9	1.3	—	—	—	—
3L1G	9.5	2.6	8.0	2.0	11.3	3.1
3L2G	11.8	3.0	−9.5	2.1	23.6	4.6

vol.40, no.1, pp.118–124, Jan. 1993.

[3] J.-H. Chern, J. Huang, L. Arledge, P.-C. Li, and P. Yang, "Multilevel metal capacitance models for CAD design synthesis systems," IEEE Electron Device Lett., vol.13, no.1, pp.32–34, Jan. 1992.

[4] S.-C. Wong, G.-Y. Lee, and D.-J. Ma, "Modeling of interconnect capacitance, delay, and crosstalk in VLSI," IEEE Trans. Semicond. Manuf., vol.13, no.1, pp.108–111, Feb. 2000.

[5] M.I. Elmasry, "Capacitance calculations in MOSFET VLSI," IEEE Electron Device Lett., vol.EDL-3, no.1, pp.6–7, Jan. 1982.

[6] C.P. Yuan and T.N. Trick, "A simple formula for the estimation of the capacitance of two-dimensional interconnects in VLSI circuits," IEEE Electron Device Lett., vol.EDL-3, no.12, pp.391–393, Dec. 1982.

[7] N. v. d. Meijs and J.T. Fokkema, "VLSI circuit reconstruction from mask topology," Integration, vol.2, no.2, pp.85–119, 1984.

[8] E. Barke, "Line-to-ground capacitance calculation for VLSI: A comparison," IEEE Trans. Comput.-Aided Des. Integr. Circuits Syst., vol.7, no.2, pp.295–298, Feb. 1988.

[9] E. Bogatin, "Design rules for microstrip capacitance," IEEE Trans. Compon. Hybrids Manuf. Technol., vol.11, no.3, pp.253–259, Sept. 1988.

[10] N.D. Arora, K.V. Raol, R. Schumann, and L.M. Richardson, "Modeling and extraction of interconnect capacitances for multilayer VLSI circuits," IEEE Trans. Comput.-Aided Des. Integr. Circuits Syst., vol.15, no.1, pp.58–67, Jan. 1996.

[11] A. Todoroki, http://florida.mes.titech.ac.jp/rec-res.html

[12] G.E.P. Box and N.R. Draper, Empirical model-building and response surfaces, John Wiley & Sons, 1987.

[13] I.N. Vuchkov and L.N. Boyadjieva, Quality improvement with design of experiments, Kluwer Academic Publishers, 2001.

[14] International technology roadmap for semiconductors: Semiconductor Industry Association, 2003.

[15] Raphael version 2004.06, Synopsys Corporation.

Atsushi Kurokawa received the B.E. degree in electrical engineering from Seikei University, Tokyo, Japan, in 1986 and the D.E. degree in information, production and systems engineering from Waseda University, Fukuoka, Japan, in 2005. From 1986 to 2002, he was with Sanyo Electric Co., Ltd., Gunma, Japan. He is now with Semiconductor Technology Academic Research Center (STARC). His research interests include high-speed/low-power design techniques and timing analysis for VLSI circuits. Dr. Kurokawa is a member of IPSJ and IEEE.

Masanori Hashimoto Masanori Hashimoto received the B.E., M.E. and Ph.D. degrees in Communications and Computer Engineering from Kyoto University, Kyoto, Japan, in 1997, 1999, and 2001, respectively. Since 2001, he was an Instructor in Department of Communications and Computer Engineering, Kyoto University. Since 2004, he has been an Associate Professor in Department of Information Systems Engineering, Graduate School of Information Science and Technology, Osaka University. His research interest includes computer-aided-design for digital integrated circuits, and high-speed circuit design. Dr. Hashimoto is a member of IEEE, ACM and IPSJ.

Akira Kasebe received the B.E. degree in electrical engineering from Nippon Bunri University, Oita, Japan, in 2001. From 2001, he is with Meitec Corporation, where he is engaged in the print circuit board design and the parasitic extraction technology development of VLSI interconnects.

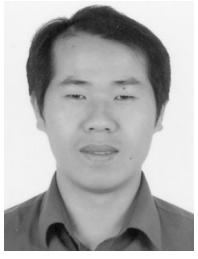

Zhangcai Huang was born on March 8th, 1978 in Jiangxi province, China. He received the B.E. degree in electrical engineering from East China JiaoTong University, Nanchang, China, in 2001. He received M.E. degree in electronic engineering from Shanghai Jiao Tong University, Shanghai, China, in 2004. He is now pursuing the Ph.D. degree at Graduate School of Information, Production and Systems, Waseda University, Kitakushu, Japan. His research interests include Static Timing Analysis, interconnect analysis and analog circuits design.

Yun Yang received the B.S. degree in electronic engineering from Fudan University, Shanghai, China, in 1998 and the M.S. degree in Micro-Electronics Department from Fudan University, Shanghai, China, in 2004. Now he is pursuing the Ph.D. degree at Graduate School of Information, Production and Systems, Waseda University, Kitakyushu, Japan. His research interests include pipeline operation, MPEG chip design, VLSI CAD development and analog/digital circuit design.

Yasuaki Inoue was born in Niigata, Japan, on September 6, 1945. He received a diploma from the Department of Electronics, Nagaoka Technical High School, Niigata, Japan, in 1964 and the D.E. degree in electronics and communication engineering from Waseda University, Tokyo, Japan, in 1996. From 1964 to 2000, he was with Sanyo Electric Co., Ltd., Gunma, Japan, where he was engaged in research and development in analog integrated circuits and analog/digital CAD systems. In Sanyo Semiconductor Company, he was General Manager of the CAD Engineering Department from 1993 to 1998 and the Memory Development Department from 1998 to 2000. He holds over forty patents. From 2000 to 2003, he was a Professor with the Department of Integrated Cultures and Humanities, also a Professor with the Graduate School of Integrated Science and Art, University of East Asia, Shimonoseki, Japan. Since 2003, he has been a Professor with the Graduate School of Information, Production and Systems, Waseda University, Kitakyushu, Japan. His research interests include numerical analysis of nonlinear circuits and systems, analog circuits, and LSI CAD systems. He was an Associate Editor of the IEEE Transactions on Circuits and Systems Part II from 1997 to 1999. He received the Ishikawa Award from the Union of Japanese Scientists and Engineers in 1988, the Distinguished Service Award from the Science and Technology Agency, the Japanese Government in 1999, the TELECOM System Technology Award from the Telecommunications Advancement Foundation in 2002, the Achievement Award from the Information Processing Society of Japan (IPSJ) in 2003, and the Funai Information Technology Prize from the Funai Foundation for Information Technology in 2004. Dr. Inoue is a member of IEEE, IPSJ, IEEJ and JSST.

Ryosuke Inagaki received the B.E. degree in electronic engineering from Osaka Institute of Technology, Osaka, Japan in 1987. From 1987, he was with ROHM corporation, where he was engaged in bipolar analog circuit design. From 2004, he is a physical researcher in STARC (Semiconductor Technology Academic Research Center). He is a visiting associate professor of Hiroshima University, Japan, in 2005. He is now pursuing the Ph.D. degree at Graduate School of Information, Production and Systems, Waseda University, Kitakyushu, Japan. He is currently interested in CMOS compact modeling HiSIM (Hiroshima University SATRC IGFET Model).

Hiroo Masuda received the B.S. degree in applied physics and Dr. of Engineering in electric system from Tokyo Institute of Technology, Tokyo, in 1970 and 1979, respectively. In 1970, he joined Central Research Laboratory, Hitachi, Ltd., Tokyo, Japan. He initially engaged in research and development of 3-μm MOS device and process. From 1975 he joined MOS memory group and developed a 64K Dynamic Memory. From 1981 to 1982 he was a Visiting Scholar at the University of Michigan, Ann Arbor. From 1982 to 1991, he was with Central Research Laboratory, Hitachi, Ltd., where he worked on semiconductor device simulation and modeling. From 1991 to 2000, he is with Device Development Center, Hitachi Ltd., where he worked on Computer Aided Engineering for VLSI's, including TCAD (Technology CAD) application methodology and statistical yield modeling and metrology. Since 2000, he is with STARC (Semiconductor Technology Academic Research Center), Development Department-1, Physical Design Group as a Senior Manage, where he is engaged in research and development works on physical design issues for sub-100 nm VLSIs. Dr. Masuda is a senior member of the Institute of Electrical and Electronics Engineers Inc., and a member of the Japan Society of Applied Physics.